CARDIOMAG NEWSLETTER

Volume 6| Issue 47| 2025

IN THIS ISSUE

Dear Doctor,

Greetings from Micro Labs Limited. We are happy to bring you "Cardio Mag" which contains latest and interesting news in the field of Cardiology

Applicability of echocardiographic strain on cardiac computerized tomographic angiography cine clips

Cardiovascular disease

INTRODUCTION- Cardiac computed tomography angiography (CCTA) is the gold standard for non-invasive coronary artery assessment.[1] While it effectively visualizes anatomical details, its role in evaluating functional myocardial implications remains underexplored. Myocardial strain analysis, particularly global longitudinal strain (GLS) and global circumferential strain (GCS) has emerged as a valuable tool for assessing myocardial deformation and subtle impairments in left ventricular (LV) systolic function. Studies have validated strain analysis using Velocity Vector Imaging (VVI) (Siemens, Mountain View, CA, USA) on steady-state free precession (SSFP) MRI cine images in hypertrophic cardiomyopathy patients. Additionally, research suggests that individuals with severe valvular heart disease may benefit from CT-based strain analysis using commercially available software. Feature tracking echocardiography has gained popularity for assessing both global and regional LV function. Given these advancements, this study investigates the feasibility of applying echocardiographic strain analysis to CCTA cine clips and explores the relationship between global and regional strain parameters and coronary stenosis severity.[2]

METHODS- This retrospective study enrolled 61 consecutive patients referred for ambulatory CCTA, primarily for coronary artery disease (CAD) exclusion. The cohort was assessed for CT segmentation consistency and VVI-generated parameters. To validate feature-tracking on CCTA cine images, 26 patients with normal LV function (EF ≥ 50%) and minimal coronary disease (calcium score <10 AU, narrowing <35%) were compared to age- and sex-matched healthy echocardiographic controls. CCTA was performed with a Philips 256 iCT scanner using a dose-reduction protocol, acquiring 20-phase cine loops for functional and strain analysis. LV cine clips in echocardiographic views were analyzed offline with VVI, which calculated global and regional strain, segmental motion, and LV volumes (Ejection fraction (EF), left ventricle end systolic volume (LVESV), left ventricular end diastolic volume (LVEDV). Patients were grouped by CCTA-determined coronary stenosis: <50% narrowing (n=44) and ≥50% narrowing (n=16). Comparisons included calcium score, LV volume, strain metrics, and rotation displacement. Regional strain was analyzed using AHA segmentation, grading stenosis as 0 (no narrowing), 2 (<50%), and 3 (50–100%), revealing an inverse relationship between strain and stenosis severity. Comparisons between groups were performed using ANOVA, and correlation analyses were conducted for volumetric and strain parameters. A p-value <0.05 was considered statistically significant.

RESULTS- In this study, patients who were included had a mean age of 55 ± 12 years, with a male predominance (59%). Patients with significant CAD exhibited a higher coronary calcium score (403 ± 422 Agatston Units) compared to the non-significant CAD group (107 ± 229, p=0.001). The median LVEDV derived from CT was 160 mL (IQR 132–181), while the

LVESV was 62 mL (IQR 53–83). The LVEF was 59% (IQR 55–66, range 42–82 mL). Moderate correlations were observed between automatically segmented 3D CT and biplane VVI-tracked volumes, with stronger correlations for LVESV than for LVEDV. The average coronary artery calcium score was 0.6 ± 1.7 (CI −1.3 to 1.3), with extra-luminal plaques in 3 subjects. CT LVEF was ≥50%, with no regional wall motion abnormalities. Among 52 age- and gender-matched echocardiographic controls, CT-derived longitudinal strain was slightly lower, while circumferential strain was higher, and both are statistically significant. Basal and apical circumferential strains were similar, but mid-level strain was higher in the CT group. Rotation displacement and systolic rotation direction were preserved across groups. LVEDV was slightly higher in the significant CAD group (163 ± 33 vs. 155 ± 30, p = ns). LVEF was lower in the CAD group, but only VVI-derived LVEF was statistically significant (59 ± 6 vs. 50 ± 11, p = 0.0002). CT-derived EF was higher than VVI-calculated EF. GLS and GCS were significantly lower in the significant CAD group, with a greater decline in GLS. Longitudinal strain was also reduced across LV regions and coronary territories. Peak circumferential strain was lower in all views except the apical. Rotation displacement angles and direction showed no significant differences between groups. Following the allocation of the segmental grading system according to coronary obstruction, 756 were normal, 268 had <50% narrowing, and 37 had ≥50% narrowing. Segmental strain decreased progressively with greater narrowing, with significant differences between the no-narrowing group and the other two groups (Figure 1).

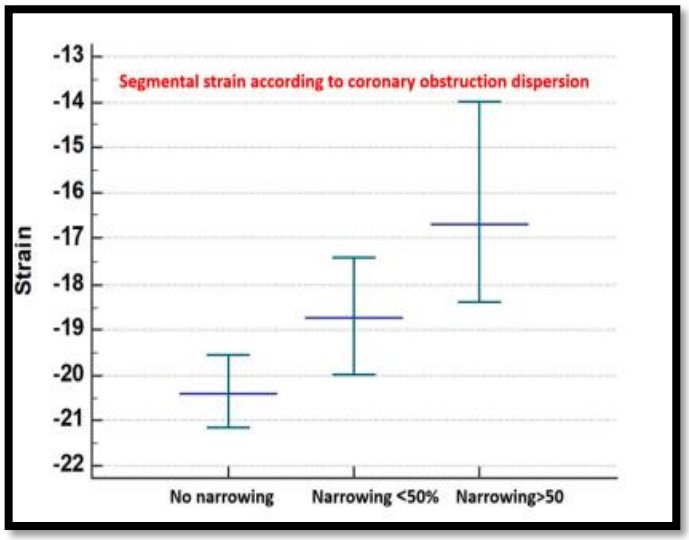

Figure 1. Segmental Strain According to Coronary Obstruction

DISCUSSION- The findings highlight significant differences in GLS and GCS between these groups, emphasizing the diagnostic value of strain imaging derived from CCTA for identifying myocardial dysfunction.[2] It was consistent with the prior studies conducted by Lamash Y et al.[3] and Peled Z et al.[4], which validated CCTA strain imaging for detecting myocardial dysfunction and early functional impairment in coronary stenosis.

CONCLUSION- Patients with severe coronary stenosis had decreased longitudinal and circumferential contraction, but the LVEF calculated from CT segmentation did not differ between groups. This implies that using VVI to follow CCTA cine clips may aid in distinguishing between substantial and non-significant coronary stenosis, giving CCTA anatomic findings more useful information.

By applying VVI to CCTA cine clip tracking, it may be possible to distinguish between significant and non-significant coronary stenosis, giving CCTA anatomic findings more useful information.

REFERENCES

1. Widmer RJ et al. Cardiac Computed Tomography Angiography in the Evaluation of Coronary Artery Disease: An Interventional Perspective. J Soc Cardiovasc Angiogr Interv. 2024 Mar 26;3(3Part B):101301.
2. Hertz A et al. Functional myocardial assessment in cine cardiac computerized tomographic angiography using echocardiographic feature-tracking software in patients with and without significant coronary disease. Int J Cardiol Heart Vasc. 2024 Dec 28;56:101586.
3. Lamash Y et al. Strain analysis from 4-D cardiac CT image data. IEEE Trans Biomed Eng. 2015 Feb;62(2):511-21.
4. Peled Z et al. Automated 4-dimensional regional myocardial strain evaluation using cardiac computed tomography. Int J Cardiovasc Imaging. 2020 Jan;36(1):149-159.

Impact of Non-Alcoholic Fatty Liver Disease on Abdominal Aortic Aneurysm Progression

INTRODUCTION- Non-alcoholic fatty liver disease (NAFLD) is a leading cause of chronic liver disease globally and is characterized by hepatic steatosis when no other causes of secondary hepatic fat accumulation (e.g., excessive alcohol consumption) can be found.[1] NAFLD is a prevalent metabolic disorder closely linked to systemic conditions such as diabetes, obesity, and cardiovascular diseases. Recent studies highlight the association between NAFLD and arterial stiffness, inflammation, and oxidative stress, all of which may influence the progression of abdominal aortic aneurysms (AAAs). Despite growing evidence, the role of NAFLD as a predictor of AAA progression remains underexplored. So, this study aimed to assess the association between NAFLD, identified via non-enhanced computed tomography (CT), and AAA progression using data from multiple medical centers.[2]

METHODS- This multicenter retrospective study included 151 patients diagnosed with AAA who underwent abdominal CTA and non-enhanced CT between January 2015 and January 2023. Patients who had a non-enhanced abdominal CT examination and the availability of a follow-up CTA scan at least six months following the initial CTA examination were included. Based on abdominal CT results, patients with AAA were categorized as non-progression and progression (growth rate >10 mL/year), as well as NAFLD and non-NAFLD. CT and CTA scans were performed using standardized protocols across participating centres. Univariate and multivariate Cox regression analyses were conducted to identify factors associated with AAA progression. Receiver operating characteristic (ROC) curves were used to evaluate diagnostic performance, and Kaplan-Meier survival curves were plotted to compare progression rates.

RESULTS- The study population had a mean age of 69.1 ± 10.5 years, with 88.1% being male. NAFLD prevalence was significantly higher in the AAA group compared to controls (43.7% vs. 31.1%, $p = 0.024$). Hypertension (62.9% vs. 51.0%, $p = 0.036$) and diabetes (28.5% vs. 15.9%, $p = 0.009$) were also more prevalent in the AAA group, while BMI and smoking history showed no significant differences. Over a median follow-up of 10.7 months (range: 6.0–76.0 months), 57 patients (37.7%) experienced AAA progression (growth rate > 10 mL/year). Progression was more frequent in patients with NAFLD (77.2% vs. 23.4%, $p < 0.001$) and was associated with larger aortic diameter [45.6 mm vs. 37.5 mm, $p < 0.001$], greater AAA volume [65.2 mL vs. 41.2 mL, $p < 0.001$], higher intraluminal thrombus (ILT) prevalence (94.7% vs. 83.0%, $p = 0.035$) and larger ILT maximal diameter [12.3 mm vs. 6.7 mm, $p < 0.001$]. Patients with NAFLD had significantly lower progression-free survival rates (log-rank

p < 0.001) (Figure 1). Univariate Cox regression identified NAFLD (HR: 5.99; p < 0.001), AAA maximal diameter (HR: 1.07 per mm; p < 0.001), AAA volume (HR: 1.01 per mL; p < 0.001), and ILT maximal diameter (HR: 1.06 per mm; p < 0.001) as predictors. Multivariate analysis confirmed NAFLD (HR: 4.28; p < 0.001) and AAA diameter (HR: 1.06 per mm; p = 0.010) as independent predictors. For predicting AAA progression, the AUCs were 0.769 for NAFLD, 0.793 for AAA maximal diameter, and 0.857 for the combined model. Sensitivity and specificity were 77.2% and76.6% (NAFLD), 80.7% and 71.3% (AAA diameter), and 73.7% and 85.1% (combined) respectively. The combined model had a significantly higher AUC than NAFLD (p<0.001) and AAA diameter (p=0.034), while NAFLD and AAA diameter showed no significant difference (p=0.608). Cohen's kappa values for intra-observer agreement were 0.917 (ILT) and 0.933 (NAFLD), while inter-observer values were 0.930 and 0.906, respectively. The intraclass correlation coefficients for maximal aneurysm diameter, total aneurysm volume, ILT maximal diameter, and growth rate ranged from 0.963 to 0.982 for intra-observer agreement and 0.954 to 0.977 for inter-observer agreement.

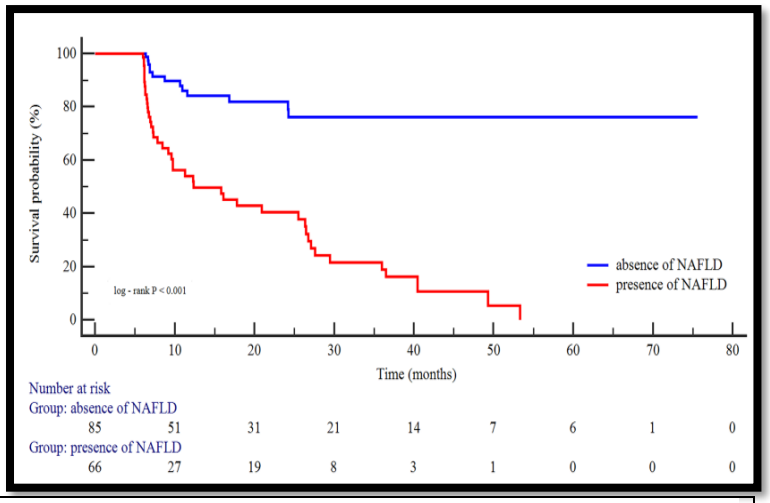

Figure 1. Kaplan-Meier event-free survival curves for AAA progression events in patients.

DISCUSSION- The current study demonstrated that NAFLD is an independent predictor of AAA progression. Additionally, the combined model incorporating AAA maximal diameter and NAFLD provided superior predictive accuracy for AAA progression, as evidenced by an AUC of 0.857.[2] These findings align with previous studies, which also reported a significant association between NAFLD and cardiovascular conditions. For instance, Mahamid et al. observed that patients with AAA had a higher prevalence of NAFLD compared to healthy controls.[3]

CONCLUSION- There was a connection between the occurrence and development of AAA and NAFLD. This study found that the maximum diameter of AAA and NAFLD were separate predictors of the AAA development. Therefore, NAFLD based on CT could be non-invasive, dependable, and simple marker to predict the course of AAA.

NAFLD upon non-enhanced CT is an independent predictor of abdominal aortic aneurysms progression.

REFERENCES

1. Pouwels S et al. Non-alcoholic fatty liver disease (NAFLD): a review of pathophysiology, clinical management and effects of weight loss. BMC Endocr Disord. 2022 Mar 14;22(1):63.
2. Wang X et al. Association between non-alcoholic fatty liver disease and progression of abdominal aortic aneurysm: a multicenter study. BMC Med Imaging. 2025 Jan 20;25(1):24.
3. Mahamid M et al. The interplay between abdominal aortic aneurysm, metabolic syndrome and fatty liver disease: a retrospective case-control study. Diabetes Metab Syndr Obes. 2019;12:1743–9.

Relationship between Triglyceride-Glucose Index and Contrast-Induced Nephropathy in Patients Undergoing Percutaneous Coronary Intervention for Chronic Total Occlusion

INTRODUCTION- The occurrence of coronary artery disease is rising with increasing life expectancy and the elderly population, leading to necessity of percutaneous coronary intervention (PCI) and coronary angiography (CAG) for chronic total occlusion (CTO).[1] A significant complication of PCI is contrast-induced nephropathy (CIN). Recently, researchers have been examining whether certain metabolic indicators may improve CIN risk categorization. The triglyceride-glucose (TyG) index has been considered a measure of insulin resistance and metabolic state. [2] Although its predictive value for CIN in selected populations has been demonstrated, limited evidence regarding its role in CTO patients undergoing PCI. So, this study assessed the association between the TyG index and the development of CIN and mortality in this population.

METHODS - This multicenter, retrospective, cross-sectional study included 218 patients who underwent procedural coronary angiography (CAG) and PCI for CTO lesions in at least one coronary artery. Patients were divided into two groups based on their TyG index: Group 1 (TyG index ≥8.65) and Group 2 (TyG index <8.65). This threshold was established based on previous studies assessing the relationship between TyG index and CIN. The inclusion criteria were adults aged 18–90 years with ejection fraction (EF) ≥40% and at least one CTO lesion requiring PCI. The primary outcomes were the development of CIN and all-cause mortality over a 96-month follow-up period. Logistic regression identified CIN predictors, including variables with $p \leq 0.1$ in univariate analysis. Kaplan-Meier analysis assessed the association of the TyG index with CIN and mortality. ROC curves determined the TyG index cutoff for CIN prediction. A p-value < 0.05 was considered statistically significant.

RESULTS – In this study, the mean age of Group 1 was significantly higher than Group 2 (65.8 ± 10.94 vs. 61.68 ± 11.4 years, $p = 0.009$). Diabetes mellitus (44.8% vs. 13.1%, $p < 0.001$) and dyslipidemia (38.8% vs. 25%, $p = 0.036$) were also more prevalent in Group 1. Other notable differences included higher rates of cerebrovascular disease (4.5% vs. 0%, $p = 0.049$) and in-stent restenosis (16.4% vs. 7.1%, $p = 0.046$) in Group 1. Biochemical analyses revealed that glucose ($p < 0.001$), triglycerides ($p < 0.001$), and uric acid levels ($p = 0.044$) were significantly elevated in Group 1. No significant differences were observed between the groups for ejection fraction (EF), hypertension, smoking status, chronic kidney disease, or peripheral artery disease. Univariate logistic regression analysis identified several predictors of CIN, including age, chronic kidney disease (CKD), peripheral artery disease, left ventricular ejection fraction (LVEF), LDL cholesterol, and the TyG index ($p < 0.05$ for all). The ROC analysis identified a TyG index cutoff of 8.86 for predicting CIN, with a sensitivity of 59% and specificity of 54% (AUC = 0.60, 95% CI: 0.51–0.68, $p = 0.044$) (Figure 1). Kaplan-Meier survival analysis demonstrated a significant association between CIN and mortality (Log-rank = 19.409, $p < 0.001$), while no significant relationship was observed between the TyG index and mortality (Log-rank = 0.808, $p = 0.369$).

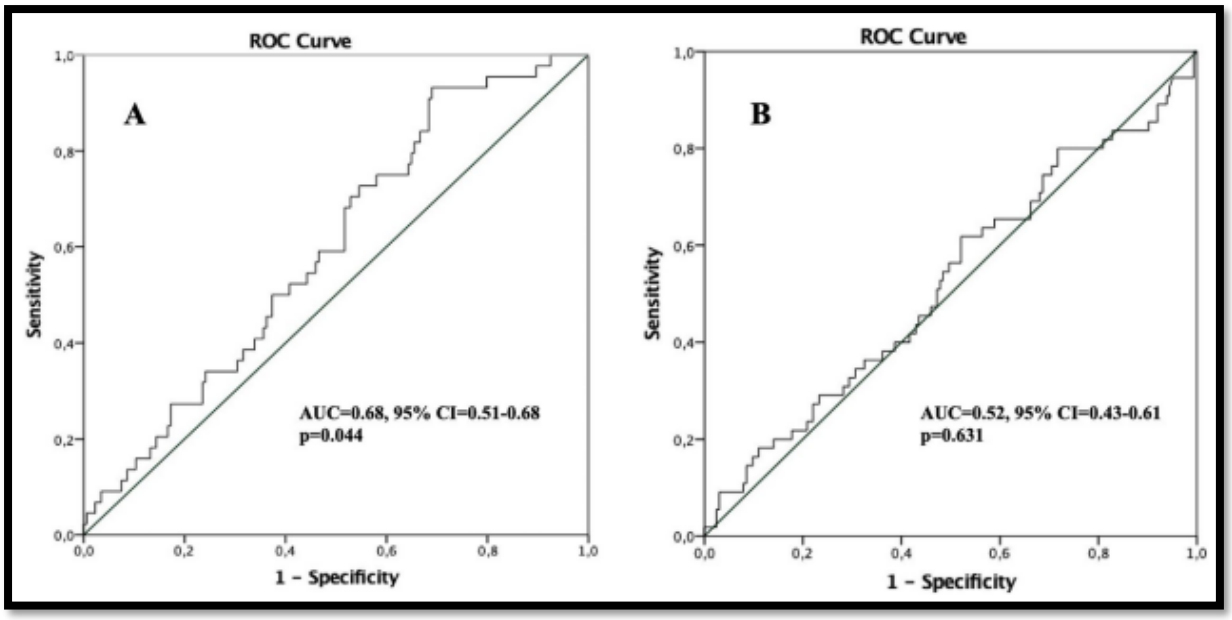

Figure 1. ROC curve analysis of TyG index to predict the development of CIN (A) and death (B)

DISCUSSION-This study demonstrated that a higher TyG index is an independent predictor of CIN in CTO patients undergoing PCI, aligning with prior studies that reported similar findings in different patient groups.[1] Qin Y et al. observed a significant association between the TyG index and CIN in patients with type 2 diabetes and coronary artery disease[3], while Gursoy E et al. noted this relationship in non-ST elevation myocardial infarction patients undergoing PCI.[4]

CONCLUSION- This study concluded that the frequency of CIN in patients with CTO having PCI is correlated with the TyG index. The TyG index is a useful tool for risk stratification in clinical settings due to its affordability and simplicity of use. Patients with CTO having PCI may be protected against the development of CIN by including the TyG index in their clinical evaluation.

The development of CIN may be prevented by including the TyG index in the standard clinical evaluation of CTO patients receiving PCI.

REFERENCES

1. Söner S et al. Association between the triglyceride-glucose index and contrast-induced nephropathy in chronic total occlusion patients undergoing percutaneous coronary intervention. BMC Cardiovasc Disord. 2025 Jan 20;25(1):31.
2. Chang WT et al. Diagnostic efficacy of the triglyceride-glucose index in the prediction of contrast-induced nephropathy following percutaneous coronary intervention. Front Endocrinol (Lausanne). 2023 Nov 22;14:1282675.
3. Qin Y et al. A High Triglyceride Glucose Index Is Associated With Contrast-Induced Acute Kidney Injury in Chinese Patients With Type 2 Diabetes Mellitus. Front Endocrinol (Lausanne). 2021;22(11):522883.
4. Gursoy E, Baydar O. The triglyceride-glucose index and contrast-induced nephropathy in non-ST elevation myocardial infarction patients undergoing percutaneous coronary intervention. Medicine (Baltimore). 2023;102(2):e32629.

A Rare Case of Single coronary artery disease

INTRODUCTION- Single coronary artery (SCA) is a rare congenital defect in which just one coronary artery emerges from a single coronary ostium and supplies the entire heart. It is typically linked with other cardiac problems. SCA has a diverse manifestation, ranging from mild, non-specific symptoms to sudden cardiac death.[1] Advancements in imaging techniques, particularly multi-slice computed tomography (CT) angiography, have improved the detection and classification of these anomalies. This case report describes a rare instance of a single coronary artery with the Right Coronary Artery (RCA) arising from the distal circumflex artery, detected incidentally during non-invasive imaging for palpitations.[2]

CASE PRESENTATION-

A 63-year-old male presented for evaluation following an inconclusive treadmill stress test due to equivocal electrocardiogram (ECG) changes. His medical history was unremarkable, with no known cardiovascular risk factors or significant family history of cardiac disease or sudden cardiac death. The patient reported palpitations, but physical examination and resting transthoracic echocardiogram were unremarkable. Holter monitoring revealed fewer than 50 daily monomorphic premature ventricular beats. Given the low pre-test probability for coronary artery disease (CAD), non-invasive imaging with 64-detector-row multi-slice computed tomography (MSCT) was performed. The MSCT revealed the absence of a right coronary artery (RCA) origin from the right sinus of Valsalva (Figure 1). Instead, the RCA was found to arise anomalously from the distal left circumflex artery. The left coronary artery (LCA), including the left anterior descending (LAD) and circumflex arteries (LCX), exhibited normal origins and courses. The RCA followed a retrograde path along the right atrioventricular groove and terminated near the right sinus of Valsalva after giving off a right ventricular branch. The LAD supplied a diagonal branch to the anterior portion of the right ventricle. No significant stenoses were observed in any arterial vessels. The patient remained asymptomatic and did not require specific medical or surgical intervention.

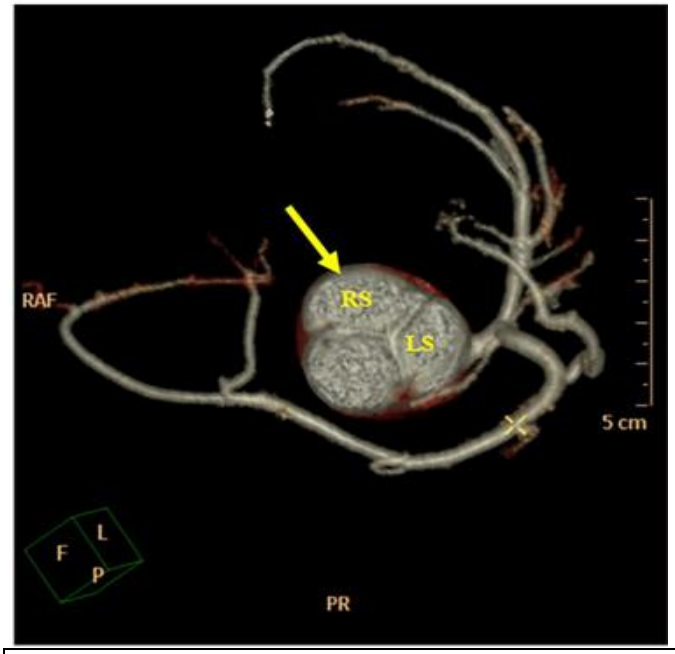

Figure 1. Single coronary artery type Lipton LI: Coronary computed tomography, volume-rendering technique (VRT) scan reconstruction: sagittal view. Right sinus (RS) left sinus (LS).

DISCUSSION- This case report highlights a rare anomaly of SCA with the RCA originating from the distal circumflex artery, classified as Lipton LI type. This anomaly, though uncommon, it is an essential consideration due to its potential clinical significance.[2] Similar findings have been documented in other case reports. Kim JM et al. reported a rare case of a 13-year-old girl with ECA originating from the left circumflex artery, emphasizing the diverse

age group in which this anomaly can present.[3] Michalowska AM et al. analysed 30,230 patients and identified 17 cases of SCA, highlighting the usefulness of CTA in identifying these anomalies. In this cohort, 35% of the cases showed SCA originating from left sinus of Valsalva, with variations in the coronary anatomy.[4]

CONCLUSION- This case study details the unintentional identification of a rare type of single coronary artery. Computed tomography angiography revealed a right coronary artery from the distal circumflex artery, which is highly helpful in patients with a low pre-test risk of coronary artery disease.

Computerized tomography angiography is very helpful in individuals with a low pre-test risk of coronary artery disease which revealed a right coronary artery from the distal circumflex artery.

REFERENCES

1. Elbadawi A et al. Single Coronary Artery Anomaly: A Case Report and Review of Literature. Cardiol Ther. 2018 Jun;7(1):119-123.
2. Mboup WN, Riviere JF. Rare Coronary Artery Anomaly: Single Coronary Artery from Distal Circumflex Detected by CT. Am J Case Rep. 2025 Jan 9;26:e946330.
3. Kim JM et al. A rare type of single coronary artery with right coronary artery originating from the left circumflex artery in a child. Korean J Pediatr. 2015;58:37-40.
4. Michalowska AM et al. Prevalence and anatomic characteristics of single coronary artery diagnosed by computed tomography angiography. Am J Cardiol. 2019;124(6):939-46.